Norway grants

Ammonia as carbon free fuel for internal CombusTion engIne driVen AgriculTural vEhicle

Work Package 1
Deliverable Report

Karl Oskar Pires Bjørgen (NTNU)
karl.o.bjorgen@ntnu.no

Topic: D1.2

Fuel injection strategy for optimized fuel mixture range

Work Package 1 leader	**Project Promoter**
David Emberson	Wojciech Adamczyk
Date 21.05.23	Date .....

Signed by / Podpisano przez:
Wojciech Piotr Adamczyk
Politechnika Śląska
Date / Data: 2023-05-22 12:41

10.05.2023

Programme operated by: NCBR National Centre for Research and Development

Project consortium: Silesian University of Technology, NTNU Norwegian University of Science and Technology, LOGE, University of Agriculture in Krakow

1 Introduction

This deliverable report reports the final outcome of the engine work that has taken place in Work Package 1 (WP1). The work has consisted in performing a systematic study on ammonia/diesel dual fuel operation on the NTNU single-cylinder test rig located at the Department of Energy and Process Engineering. The results include performance and emissions measurements for various operating points, focusing mainly on injection timing for ammonia and diesel, increasing engine load and ammonia energy share (AES). Challenges related to the use of FTIR, fuel mass estimation and repeatability are also highlighted in this report, along with a conclusion of optimal injection strategies within the tested engine operating range. The deliverable report concludes the work conducted in WP1.

1.1 Review of ammonia combustion in HPDF engines

Dual fuel engines can generally have a low reactive fuel, such as natural gas, liquid petroleum gas (LPG), methanol or ammonia, and a high reacting fuel, such as a diesel-like fuel. The high reactivity fuel is often referred to as the pilot injection fuel since it initializes the combustion process of the low reactivity fuel, which is not able to ignite solely based on the compression inside the engine cylinder. The low reactive fuel can be injected into the engine in two ways, i.e. port injected or direct injected. For port injection, the low reactivity fuel is either injected in a liquid state or in a gaseous state, and the injection pressure is typically low, i.e. in the range of 5-20 bar. This engine mode is referred to as low injection pressure dual fuel (LPDF) mode. The alternative is to inject the low-reactivity fuel directly into the cylinder as the main injection, either as a liquid or gaseous state and ignite the fuel by a pilot injection, normally injected prior to the main injection.

There have been published a handful of experimental and numerical studies on ammonia as the main fuel in high-pressure injection dual fuel (HPDF) mode. The development is rapid and new studies are being added to the literature. Therefore, a thorough and updated review is provided in this deliverable.

Frankl et al. 2021

Frankl et al. [1] investigated ammonia and diesel in HPDF mode in a low-speed marine engine numerically. The ammonia was injected directly and ignited by a small injected mass of diesel fuel. The diesel pilot injection was injected at -2.5 crank angle degrees after top dead centre (CAD aTDC), and the ammonia main injection was at 1 CAD aTDC. Assuming 750 rpm engine speed, the delay between the pilot and main injection was 0.78 ms. They also investigated the effect of injection pressure, fuel temperature, and ammonia phase state. The results show that higher injection pressure and fuel temperature positively affect ammonia combustion's heat release rate (HRR). A larger pilot injection results in earlier ignition of ammonia, but not faster combustion. Unfortunately, Frankl et al. did not report any information on emissions or unburned ammonia.

Li et al. 2022

Li et al. [2] studied HPDF and LPDF mode with ammonia and diesel numerically in a CI engine. The injector was a combined diesel and ammonia injector with 8 holes for diesel and 8 holes for ammonia. They tested two spray configurations, where the first had alternating diesel and ammonia sprays and the second had overlapping diesel and ammonia sprays. The engine speed was kept at 1000 rpm, the ammonia energy share was varied between 90 % to 99 %. For comparing the two hole

arrangements, i.e. overlapping and alternating holes, the AES was kept fixed at 97 % AES, the air intake conditions were kept constant, the diesel injection timing was held at -8 CAD aTDC, and the ammonia injection timing at -5 CAD aTDC, resulting in a delay of 0.5 ms between the pilot and main injections.

For both hole configurations, the ignition delay time of the diesel pilot injection is similar to that of pure diesel mode, while ignition of the ammonia main injection occurs approximately 4 CAD (0.67 ms) after the ignition of the pilot. The heat release rate (HRR) curve is slightly advanced for the overlapping hole arrangement compared to the alternating hole arrangement, this is due to increased interaction between the diesel pilot and the ammonia main sprays. The overlapping hole arrangement also gives lower N2O, NOx, and unburned ammonia emissions, and was concluded to yield the optimal result. The effect of changing the AES was investigated, varying the AES between 90 %, 97 %, and 99 %. The 99 % AES case did not yield ignition. The 97 % and 90 % AES cases show similar diesel pilot ignition delay times compared to the pure diesel case. The start of ignition of ammonia for the 90 % AES case occurs immediately after injection, while the 97 % AES case experiences a delay, causing a higher peak in HRR due to more time to premix the ammonia before combustion starts. N2O, NOx and unburned ammonia emissions were found to be lower for the 90 % AES case compared to the 97 % AES case.

Scharl and Sattelmayer 2022

Scharl and Sattelmayer [3] performed an experimental investigation of HPDF mode with ammonia and diesel in a rapid compression expansion machine (RCEM) with a bore of 220 mm, simulating the conditions found in an engine. The equivalent engine speed was between 800-1000 rpm, with TDC temperatures and pressures in the range 780-920 K and 75-125 bar, respectively. Two single-hole injectors for ammonia and diesel were used with maximum injection pressures of 530 bar and 2000 bar, respectively. The AES varied between 90 % and 99 %. The ammonia and diesel injectors were configured in such a way that spray interaction could be investigated by rotating the ammonia injector. Additionally, the relative injection timing of the ammonia main injection varied between -1.00 ms and 1.5 ms. The maximum ammonia injection duration was 2.7 ms, while for diesel injection it was 0.83 ms for the 0.20 mm hole diameter nozzle and 1.46 ms for the 0.11 mm hole diameter nozzle. The study was performed by varying the spray interaction between converging, parallel and diverging ammonia and diesel sprays. Meanwhile, the relative injection timing was varied.

The results show that the highest burnout rate is achieved for slightly converging sprays and when ammonia is injected 0.5 ms after the diesel injection. Misfire was observed for highly converging sprays when ammonia was injected simultaneously or before diesel. For ammonia injections occurring simultaneously or earlier than the diesel injections, increasing the AES resulted in misfires for less converging angles between the sprays compared to the higher AES case. The parallel or converging sprays, with moderately advanced diesel injection, give high burnout rates since the ignition of the diesel spray can occur undisturbed, and therefore, the ammonia spray is able to ignite and burn subsequently.

The diesel pilot ignition delay was unaffected when the ammonia injection was delayed for all spray angles and diverging spray configurations. The opposite was observed for parallel or converging sprays when ammonia was injected simultaneously, or before diesel, this is due to the strong interference of ammonia on the diesel spray. The ignition delay of the main injection is short for strong spatial interactions and advanced diesel injection, correlating well with the burnout rate, where short ignition delay times lead to a high burnout rate. For the injection of ammonia simultaneous or before the diesel injection, the relative ignition delay time between the pilot and the main is unaffected by a change

in the ammonia injection timing. At the same time, the burnout rate decreases while advancing the ammonia injection. The authors hypothesize that the increased ammonia wall interaction with advanced ammonia injections is the cause of this.

The ignition delay time of the pilot and main injections increases for low pressure/temperature charge conditions, while the lowest condition results in a misfire. Ammonia was shown to operate poorly in low-load conditions. The diesel pilot injection affected the combustion of ammonia, where the reliable ignition of ammonia was possible up to 96.8 % AES. The ammonia ignition delay increased for smaller pilot masses, and short diesel pilot injections with higher mass flow rate intensifies the ammonia combustion.

Scharl et al. 2023

In a follow-up study by Scharl et al. [4], they optically look closer into the combustion process occurring inside the RCEM. The optimal configuration found in [3] is adopted in this study, which corresponds to having an angle of -7.5 CAD between the diesel and ammonia sprays (converging) and having an ammonia injection timing of 0.5 ms after the diesel injection. The optical setup consisted of shadowgraphy, OH* chemiluminescence and planar Mie scattering imaging.

Images are collected for three injected masses of ammonia, where the injection duration is kept constant and the injection pressure is varied. The pilot injection is fixed at 5 mg diesel. The pilot injection ignites before ammonia is injected, and the ignition of ammonia starts at the same time for all three injected ammonia masses. The HRR profiles are similar for the 190 mg and 220 mg injected ammonia cases, and the 125 mg injected ammonia case shows a slower HRR development. The time when the HRR reaches the peak corresponds to the time when the ammonia spray flame reaches the wall, indicating that wall quenching has a major impact on the combustion. The OH* signals are similar for the 190 mg and 220 mg ammonia cases, while the 125 mg decays at a later stage, indicating that the former cases interact earlier with the ammonia injection. For all cases, a weak and declining OH* signal is observed during the ammonia burnout period. The flame lift-off length is observed to slowly increase for all cases during the ammonia burnout period, showing that the flame is unable to stabilize under engine-like conditions.

Zhang et al. 2023

Zhang et al. [5] performed an experimental study on the combustion of ammonia and diesel in a two-stroke low-speed engine operating in HPDF mode. The engine bore was 150 mm, having a compression ratio of 13.8, and was operated at 375 rpm. The intake air was conditioned to 27°C and 1.35 bar. The ammonia and diesel injectors were pressurized at 650 and 1000 bar, respectively. The mass of ammonia was measured by injecting ammonia into a closed container filled with water and weighing the container before and after. The two injectors' orientation is unclear from the manuscript, but the illustration might suggest that they are mounted on the head and located on opposite sides of the cylinder. As mentioned in the studies above, the spray pattern of ammonia and diesel is important.

The engine tests are organised in three campaigns, Case 1, Case 2 and Case 3. Case 1 keeps the diesel and ammonia injection timings fixed, only changing the ammonia injection duration and the injected ammonia mass, corresponding to AES of 0%, 39 %, 45 %, and 51 %. Case 2 varies the ammonia injection timing between -16 and -8 CAD aTDC with 51 % AES. Case 3 varies diesel injection timing between -12, -10, -8 and -6 CAD aTDC for 51 % AES.

For Case 1, the calculated HRR profiles show that the diesel ignition delay time and peak HRR are

not affected by the different masses of injected ammonia. The simultaneous injection of ammonia with different masses all ignite at the same time, but the peak HRR caused increases for higher energy input of ammonia. The measured emissions show that total hydrocarbon (THC), CO and soot specific masses are reduced by the addition of ammonia, while NOx increases.

Case 2, where the ammonia injection timing is changed for AES of 50 %, shows that advancing the ammonia injection does not affect the start of ignition for all cases, even though the earliest injection of ammonia occurs 3.55 ms (8 CAD) before the diesel injection. The start of ammonia combustion is analyzed in detail for the three AESs by subtracting the diesel-only HRR profile from the ammonia-diesel cases. The earliest injection of ammonia at -16 CAD aTDC yields a short ignition delay time between diesel and ammonia, but the peak HRR is lower than the two later injections, indicating that premixing ammonia prior to diesel injection is not beneficial. The simultaneous injection of ammonia and diesel at -8 CAD aTDC is regarded as an inhomogeneous premixed and diffusion combustion of ammonia. The peak HRR value is the highest for this case indicating that diffusive combustion is beneficial. The latest injection of ammonia at 0 CAD aTDC yields diffusive combustion of ammonia, however, the combustion duration is long which deteriorates the combustion efficiency, although the authors do not provide any further information on combustion efficiencies. However, the simultaneous ammonia and diesel injection case yields the highest indicated thermal efficiency, and the shortest combustion duration. The combustion duration of this case is significantly shorter than that of the equivalent diesel-only case. For emissions, the NOx emissions are highest for the best case of simultaneous injection, while is significantly reduced for the late ammonia injection case. As for THC, CO and soot, they all are lowest for the simultaneous injection, however, the differences are low.

Case 3 varies the diesel injection timing and keeps the ammonia injection fixed at -8 CAD aTDC and the AES at 50 %. The first ignition for all diesel injection timings coincides well with the diesel injection timings, showing that the ammonia injection is not interfering with the initial ignition process even for the case where ammonia is injected before diesel, i.e. diesel at -8 and ammonia -6 CAD aTDC. The combustion phasing for CA10 and CA50 for all diesel injection timings is similar to the diesel-only case, while for the CA90, i.e. the total combustion duration, the ammonia-diesel cases are all significantly longer than that of the diese-only case. The fast combustion of ammonia is attributed to the fast atomization and evaporation of ammonia compared to diesel. The indicated thermal efficiency is highest for the simultaneous (-8 CAD aTDC) diesel injection timing case. For emsissions, NOx decreases monotonically as diesel injection is delayed, and is overall higher for the ammonia-diesel cases compared to the diesel-only case. The THC, CO and soot remain unchanged for the ammonia-diesel cases.

Summary of review

The published work on dual fuel combustion of ammonia in HPDF mode is scarce, however, the mentioned studies give a clear indication that the HPDF mode for ammonia is promising. However, there has only been one experimental study published on actual engine work with DI of ammonia and diesel by Zhang et al. [5], and this study does not include unburned NH3 and N2O emission, which are identified as the biggest challenge related to ammonia combustion. They also do not provide any clear information about the combustion efficiency. This is also lacking the work performed by Scharl et al. in [3] and [4]. However, Scharl et al. conclude that the interaction between the ammonia and diesel sprays are very important for the combustion characteristics, indicating that injector orientation, ammonia spray characteristics and injection timings are very important to consider. The numerical study performed by Li et al. [2] suggests that overlapping sprays diesel and ammonia

spray reduce the N2O and unburned ammonia, further motivating Scharl and Sattelmayer's optimal configuration.

2 Methods

The engine setup developed in ACTIVATE WP1 is described in great detail in Deliverable Report 1.1, Milestone Report 1.1, 1.2 and 1.3. A short summary is provided below.

The engine test rig consists of a single-cylinder engine connected to an electric motor which acts like a motor during motoring cycles and a brake during firing cycles. The intake air can be conditioned by an intake air heater and a roots compressor. The head has been modified to fit a Bosch CR diesel injector for diesel injections, and a Bosch GDI injector for injection of ammonia. Ammonia can be injected with a max pressure of 200 bar and the mass flow rate is recorded during engine operation.

The injectors' orientation was kept the same as reported in Milestone report M1.3.

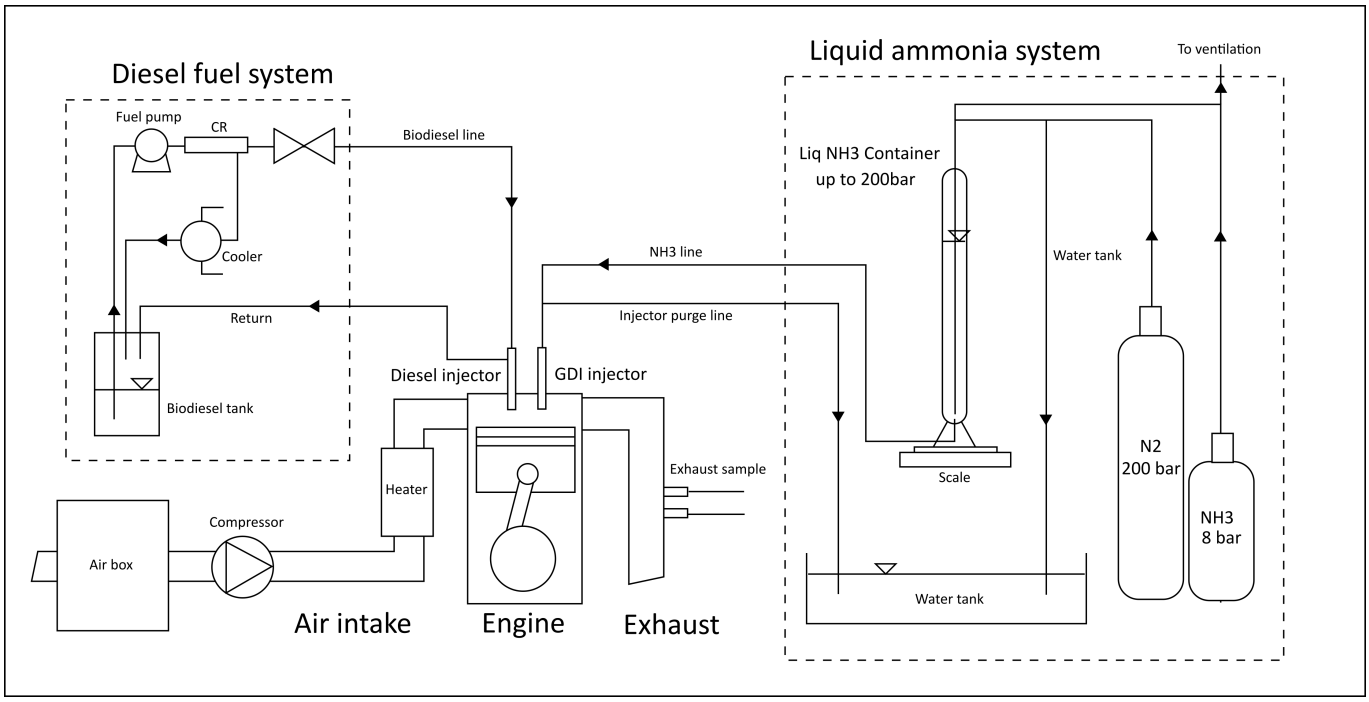

Figure 1: Schematic overview of the engine rig at NTNU.

2.1 FTIR gas analyzer

The exhaust gas concentrations of the listed gases below, in Table 1 are measured by a Fourier Transform Infrared (FTIR) gas analyzer. The CX4000 from Gasmet Technologies Oy is a portable FTIR analyzer capable of measuring multiple gas concentrations simultaneously. The FTIR gas analyzer receives a conditioned gas sample via a gas sampling system. The gas sampling system consists of a Gas Sampling Unit which is heated to 180°C, the Gas Sampling Unit pumps the gas sample from the exhaust pipe of the engine in via a heated probe (MC PSP4000H) and a heated line. The sample gas passes through a high-efficiency filter in the Gas Sampling Unit and directs the sample gas to the FTIR analyzer. The sample gas is at all times held at 180°C to avoid any condensation

of gases in the FTIR analyzer, which potentially can damage it. Each gas sample is sampled for 5 seconds continuously during the engine tests, providing an near-instantaneous measurement of gas concentrations. All concentrations are made on a wet basis, and since water is measured, the dry gas concentrations can be calculated. The FTIR analyzer raw data is analyzed by a software called Calcmet by Gasmet Technologies Oy. Calibration spectra for all gases are provided by the manufacturer, and together with a zero calibration spectrum performed before each measurement, the gas concentrations and residuals are provided.

Gas	Measuring range	Unit
Water vapor H2O	0.5-30	% vol
Carbon dioxide CO2	3-30	% vol
Carbon monoxide CO	20-20000	ppm vol
Nitrogen monoxide NO	20-500	ppm vol
Nitrogen dioxide NO2	20-100	ppm vol
Nitrous oxide N2O	20-200	ppm vol
Sulfur dioxide SO2	20-200	ppm vol
Ammonia NH3	10-10000	ppm vol
Methane CH4	10-50	ppm vol
Ethane C2H6	10-20	ppm vol
Ethylene C2H4	10-20	ppm vol
Propane C3H8	10-20	ppm vol
Hexane C6H14	5-10	ppm vol
Formaldehyde CHOH	25-45	ppm vol

Table 1: FTIR analyzer gas concentration measuring ranges.

2.2 Operating conditions

The targeted engine operating conditions are shown in Table 2. The intake air conditions were constant for all tests, i.e. 40°C and 1.2 bar. The engine speed was fixed at 1500 rpm. The energizing duration of diesel injection was 1.00 ms for all tests. The targeted injection pressure of diesel was 900 bar and 190 bar for ammonia. The constant engine speed and air intake conditions result in the same thermodynamic conditions for all tests when considering the air cycle.

Engine parameters	Target value	Unit
Engine speed	1500	rpm
Intake air pressure	1.2	bar
Intake air temperature	40	°C
Diesel injection pressure	900	bar
GDI injection pressure	190	bar
Diesel energizing duration	1.00 (9.00)	ms (CAD)
GDI energizing duration C1	1.06 (9.54)	ms (CAD)
GDI energizing duration C2	1.45 (13.08)	ms (CAD)
GDI energizing duration C3	2.05 (18.41)	ms (CAD)

Table 2: Targeted engine parameter values.

The total fuel energy and the AES for all engine runs are shown in Figure 6b. The AES is stable for most cases and is 40 %, 50 % and 60 % for conditions 1, 2 and 3 respectively. The drop observed

for the last engine runs for conditions 1 and 2 is due to high in-cylinder pressures due to the late injection of ammonia, causing less fuel to be injected for the same injection pressure.

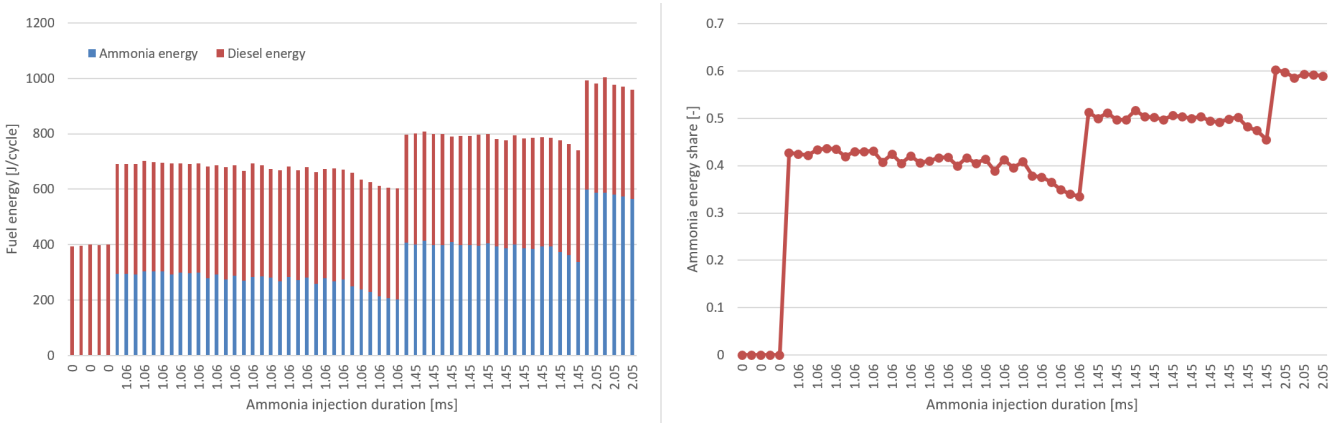

Figure 2: .

The time-averaged values for the above-mentioned engine parameters are shown in Figure 3 for all engine runs performed. The average and sample standard deviation of the engine parameters are calculated for all engine runs and shown in Table 3. This provides an indication of the variation of the values, although each calculated point also varies during the engine run time, which was 40 seconds. Each engine run consists of 1000 engine cycles, where only the last 500 cycles are recorded. This number of cycles per engine run was chosen as a compromise between maximizing the run time for attaining stable engine operation and exhaust emissions measurements, and minimizing the run time for saving ammonia fuel. For instance, for the engine runs having the longest ammonia injection duration, i.e. 2.05 ms, each engine run requires approximately 30 grams of ammonia, and with an ammonia tank containing only 300 grams of ammonia when full, this results in 10 engine runs and a total run time of 13 minutes before the tank is empty and needs a refill.

	Average	Standard deviation	Unit
P inlet [bar]	1.2005	0.0012	bar
T inlet [degC]	40.36	0.63	°C
Engine speed [rpm]	1504.29	3.79	rpm
Diesel inj p [bar]	930.72	16.39	bar
Ammonia inj p [bar]	184.23	7.02	bar

Table 3: Average values and the sample standard deviation of the engine parameters for all engine runs.

The varying parameters are the injection timing of ammonia and diesel, energizing duration of the ammonia injection and the diesel injection. An overview of the operating points performed is provided in Figure 4.

2.3 Injected mass of ammonia

The injected mass of ammonia was calculated based on the change in weight of the ammonia tank while running the engine. The method for calculating the mass flow rate of ammonia is described in M1.3. The resulting injected masses of ammonia per cycle for the three operating conditions

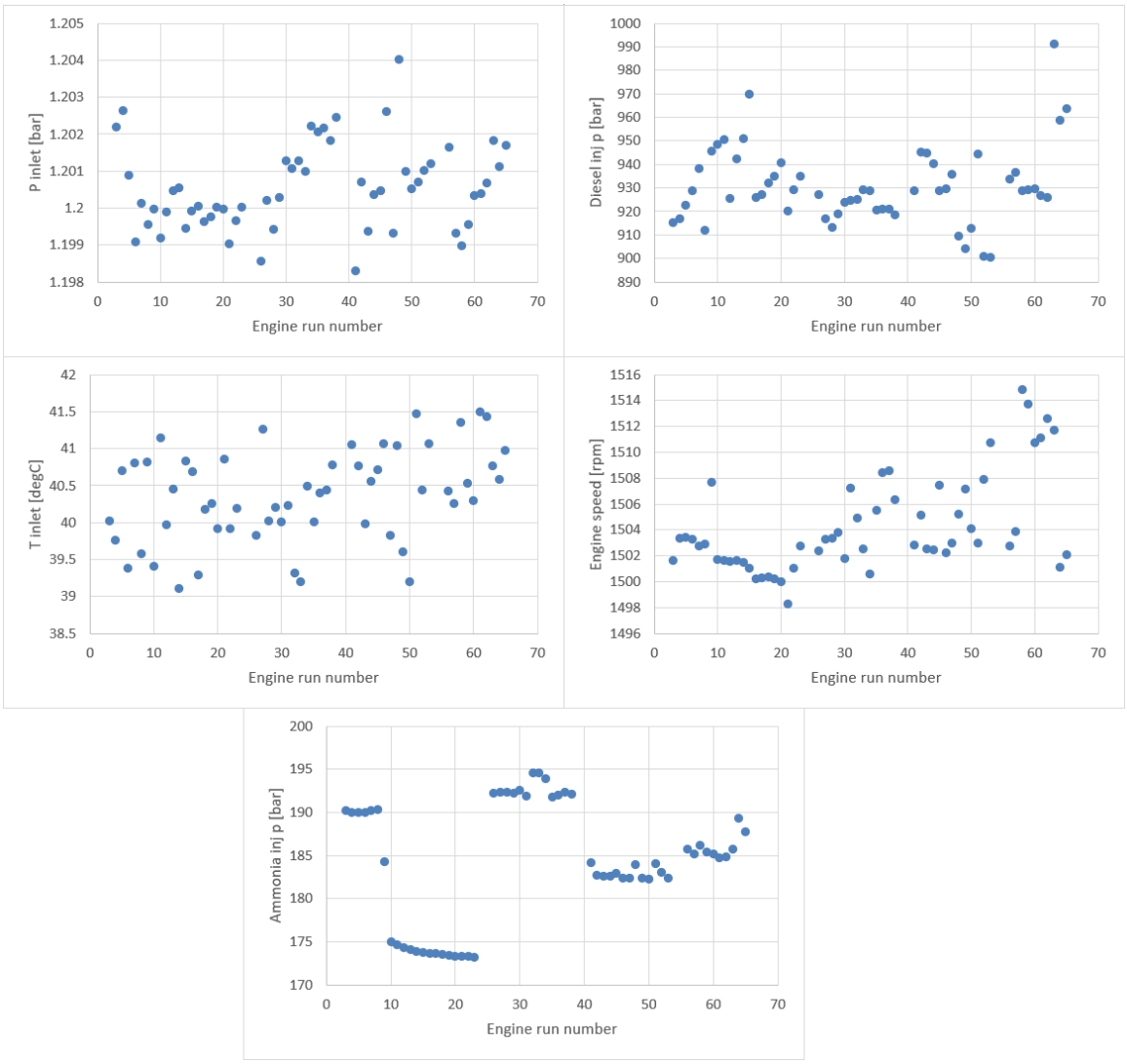

Figure 3: The engine parameters.

performed during the current measurement campaign are shown in Figure 5. The injected mass of ammonia is plotted against the square root of the injection pressure drop through the GDI injector, which is based on Bernoulli's equation, where the square root of the pressure drop through a nozzle is linear to the mass flow rate of the fluid, see Equation 1. By assuming that the shape of the mass flow rate profile for injections with the same energizing duration does not change significantly, the injected mass can be assumed proportional to the square root of the pressure drop (Equation 2).

$$\dot{m}_{inj} = A\sqrt{2\rho_f \Delta P} \tag{1}$$

$$m_{inj} \sim \sqrt{\Delta P} \tag{2}$$

The injected mass of ammonia per cycle is an important quantity since it affects the calculation of the thermal and combustion efficiencies of the engine. The measurement method used is reliant on the measured fuel pressure and temperature of ammonia in the fuel tank and the differential weight of ammonia over time and is therefore subjected to several uncertainties. In addition, even though the injection pressure is kept close to 190 bar for all tests, the in-cylinder pressure varies based on

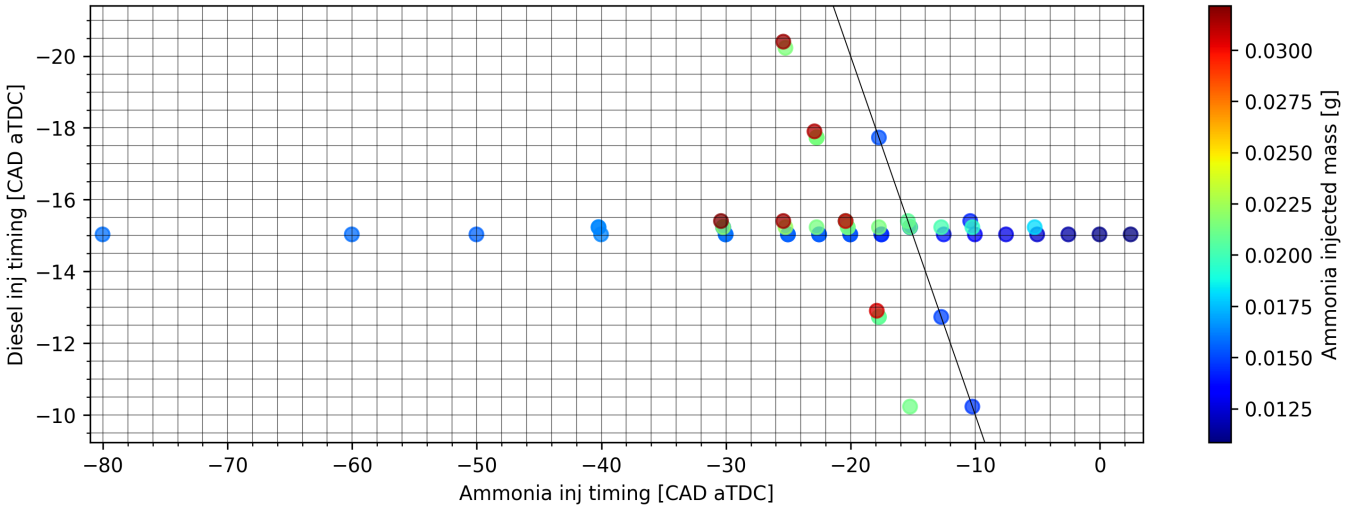

Figure 4: Ammonia mass injected and the corresponding ammonia and diesel injection timings performed.

the time of injection. For instance, when injecting early, the in-cylinder pressure can be as low as 5 bar, while if injected after the diesel injection, the pressure could be as high as 80 bar since the combustion of diesel is taking place. In order to minimize the effect of the combined uncertainties, the measured injected mass of ammonia is calculated based on all tests performed, and an empirical correlation is made, such that the effect of outliers does not affect the analyzed results. The linear regression fits displayed in Figure 5 is forced through origo and provides a correlation which is used for calculating the thermal and combustion efficiencies. By inputting the ammonia injection pressure, in-cylinder pressure and energizing duration, the injected mass can be determined.

3 Results

The results of the engine campaign performed at 0 %, 40 % and 50 % AES are presented as variations of ammonia injection timing and combustion phasing in the two following separate sections. Figure 6a shows the resulting AES of all engine operating points. The AES is relatively stable for tests performed between -80 and -15 CAD aTDC, however, delaying the injection further resulted in a decrease of AES. The injected mass of ammonia decreased for the later injections because the in-cylinder pressure was higher. This is also seen in the injected fuel energy per engine cycle in Figure 6b. The engine runs with AES 60 % are not presented in the results below since there were issues related to the emissions measurements. Be aware that the x-axis of the plots showing the injection timing combinations does not have the same CAD step size.

3.1 Effect of ammonia injection timing

Engine performance

Figure 7 shows the thermal and combustion efficiencies for AES 40 % and AES 50 % for varying ammonia injection timings with fixed diesel injection timing at -15 CAD aTDC. The results show that the thermal efficiency for AES 40 % is very low for early ammonia injection timings, i.e. 33 %, but gradually increases when delaying the ammonia injection until -30 CAD aTDC. For ammonia

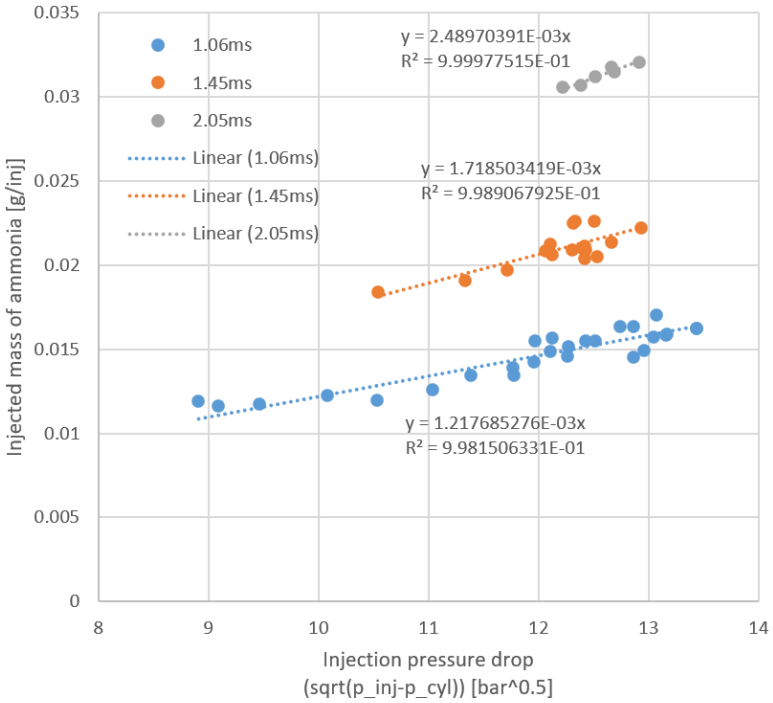

Figure 5: The injected mass of ammonia for the three operating points of the engine.

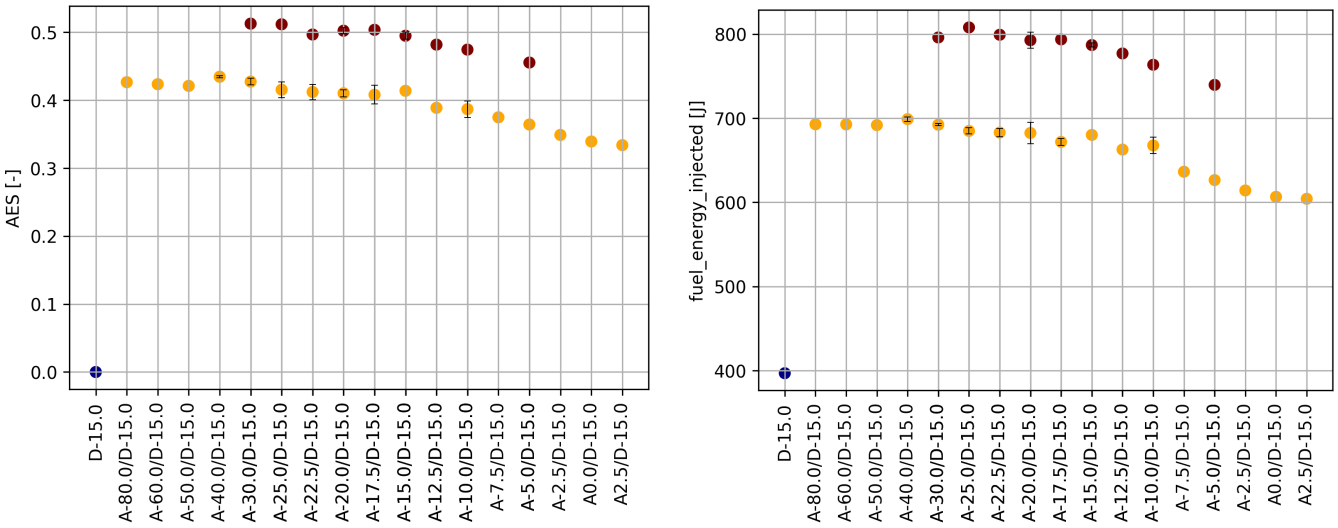

(a) Ammonia energy share.

(b) Total fuel energy injected per cycle.

injection timings between -30 to -7.5 CAD aTDC, the thermal efficiency is stable at around 38 %, similar to that of diesel. After -7.5 CAD aTDC, it increases gradually to approximately 39 CAD aTDC, this is likely due to having a lower AES for the latest ammonia injection timings, see Figure 6a. For the AES 50 % cases, the thermal efficiency decreases from -30 CAD aTDC, with earlier injection timings of ammonia being the best-performing cases. Unfortunately, an optimum of the efficiencies for the AES 50 % cases was not captured. For the combustion efficiencies shown in Figure 7b, a similar trend is found for the thermal efficiencies.

The cycle-to-cycle variation for the maximum in-cylinder pressure and the indicated mean effective

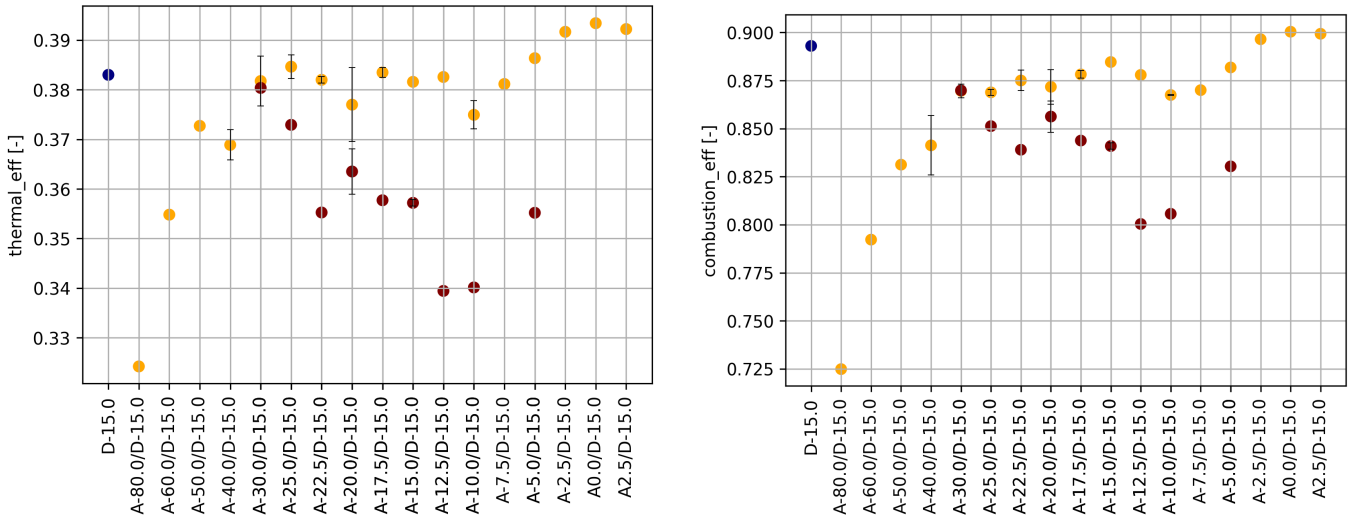

(a) Thermal efficiency.

(b) Combustion efficiency.

Figure 7: Varying ammonia injection timing while keeping diesel injection timing at -15 CAD aTDC.

pressure (IMEP) are shown in Figure 8. The coefficient of variance (COV) is calculated as the ratio between the standard deviation and the sample mean of the 500 cycles for each engine run. The IMEP COV gives an indication of the cycle-to-cycle power delivery stability, where the best operating point for the 40 % AES case yields 1 % COV IMEP, while for the AES 50 % it is 1.5 %. There is a tendency for both AES to have a more stable power delivery when injecting ammonia slightly before diesel injection, i.e. slightly before -15 CAD aTDC, indicating that this is an operating point yielding good combustion. The COV for the maximum in-cylinder pressure shows that the peak pressure is most unstable for ammonia injection timings of -30 and -25 CAD aTDC, and increases from 1.5 % to 2.5 % at -25 CAD aTDC when increasing the AES from 40 to 50 %.

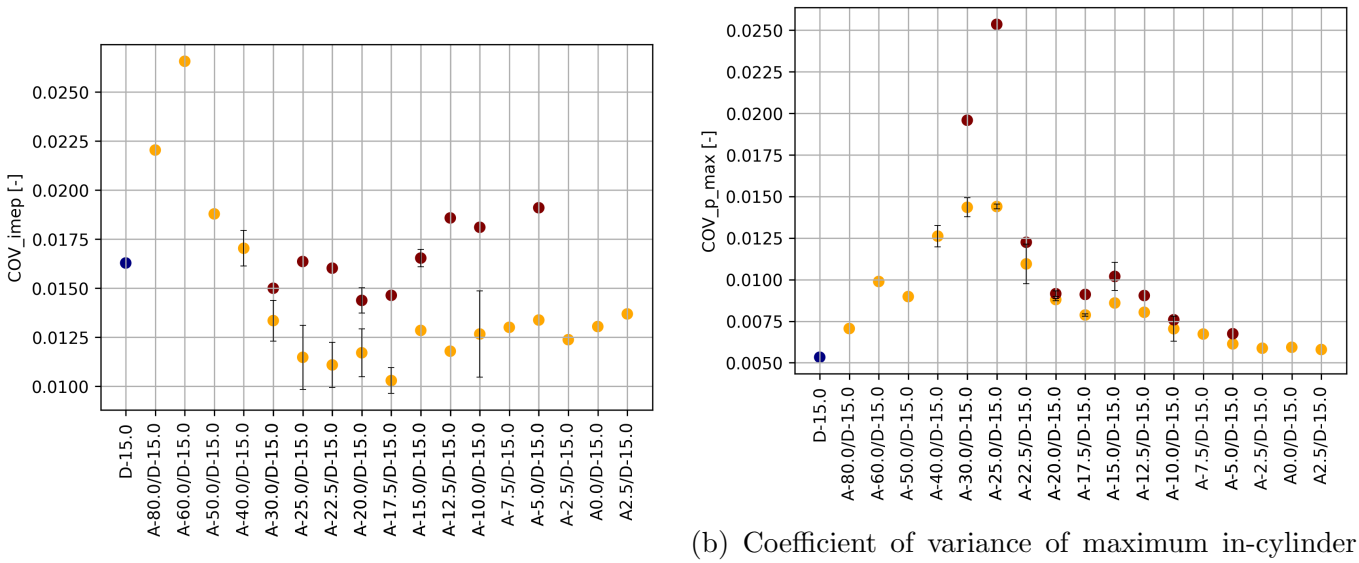

(a) Coefficient of variance of IMEP.

(b) Coefficient of variance of maximum in-cylinder pressure.

Figure 8: Varying ammonia injection timing while keeping diesel injection timing at -15 CAD aTDC.

The occurrence of 10 %, 50 % and 90 % (CA10, CA50 and CA90) of the released combustion heat

is shown in Figures 9 and 10. This shows how the combustion develops during the engine cycle. The CA10 provides an indication of the start of combustion and is closely linked with the start of ignition. The figures also show the diesel-only case, indicating that CA10 of diesel occurs at -9 CAD aTDC, i.e. approximately 0.6 ms after the start of diesel injection. As ammonia is injected early at -80 CAD aTDC, the ignition is delayed due to the influence of the presence of ammonia and the reduced in-cylinder temperature, resulting in a CA10 being at -6.5 CAD aTDC, i.e. 0.95 ms. The CA10 is delayed further as the injection of ammonia is delayed and reaches the maximum at -25 CAD aTDC for AES 40 %, at -4 CAD aTDC, corresponding to 1.22 ms from the start of diesel injection. The peak indicates considerable interaction between the ammonia and diesel sprays for these injection timings. The CA10 thereby decreases for later injection timings of ammonia. Injecting ammonia after -15 CAD aTDC, i.e. injecting after the start of diesel injection, results in an unaffected ignition of diesel. However, the CA10 is delayed by 1 CAD for AES 40 % and 2 CAD for AES 50 % compared to that of diesel. This could be explained by the thermodynamic conditions in the cylinder being affected by the previous combustion cycles. The CA50 gives an indication of the combustion phasing, showing when 50 % of the heat is released during the cycle. For both AESs, the CA50 reaches a minimum close to -22 and -20 CAD aTDC. CA90 indicated the end of the combustion. For both AESs, the combustion cycle ends at between -17 and -25 CAD aTDC for the stable operating points, while injecting ammonia after -15 CAD aTDC extends the combustion duration. For AES 40 % when delaying the ammonia injection timing after -17.5 CAD aTDC, there is a near monotonical increase, except for a plateau occurring between -12.5 and -7.5 CAD aTDc. A similar trend is found for AES 50 %.

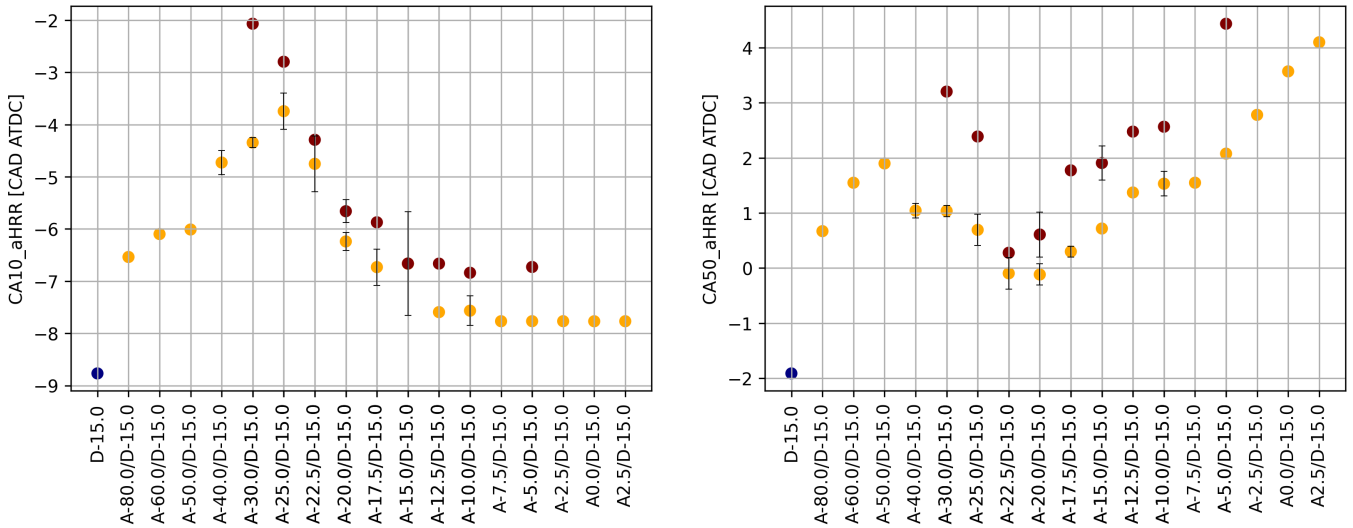

(a) Combustion progression position of 10 % heat released.

(b) Combustion progression position of 50 % heat released.

Figure 9: Varying ammonia injection timing while keeping diesel injection timing at -15 CAD aTDC.

The calculated mean heat release curves of the engine runs performed for AES 40 % are presented in Figure 11. The figure compares the diesel-only case with ammonia-diesel cases. Injecting ammonia at -80 CAD aTDC causes the ignition to be slightly delayed compared to that of diesel-only. Injecting ammonia at -60 and -40 CAD aTDC results in a premixed combustion phase being observed, with a following diffusion-based flame. This is likely because the ammonia has time to mix and vaporize in the air before diesel is injected, igniting the mixture. Figure 13 shows the total heat energy released

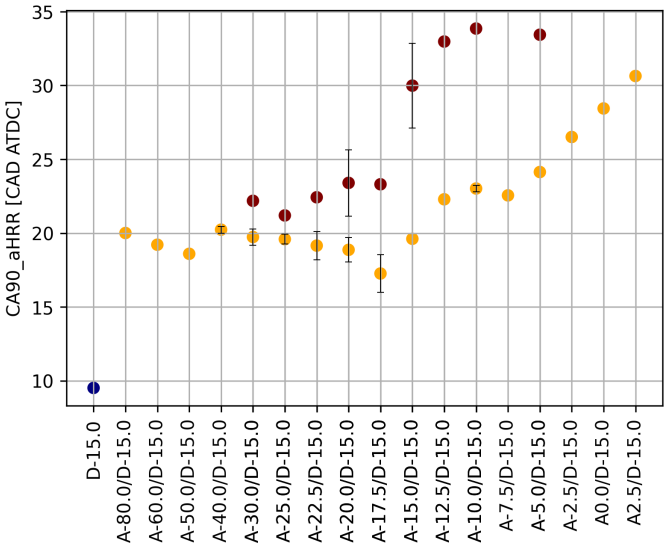

Figure 10: Combustion progression position of 90 % heat released.

during each cycle for AES 40 % and 50 %. The heat energy released for AES 40 % increases gradually from -80 to -30 CAD aTDc, reaching a plateau for injection after -30 CAD aTDC. Additionally, a clear transition occurs between -30 to -20 CAD aTDC, where the diesel premixed phase is observed for -30 CAD aTDC and -20 CAD aTDc, but not for the -25 and -22.5 CAD aTDC. The two injection timings in between show a heavily premixed combustion mode, with a high HRR peak and a very delayed ignition start, as observed in the CA10 figure above. The COV of peak in-cylinder pressure also showed a high value for these two injection timings, indicating a fluctuating heat release rate peak, typical of premixed combustion. The tipping point at approximately -25 CAD aTDC indicates that the ammonia spray is influencing the diesel spray significantly, cooling the surroundings of the diesel to such a degree that ignition is hampered. The cooling causes diesel and ammonia to mix properly before ignition, resulting in premixed combustion. As the injection of ammonia is further delayed, the diesel experiences less ammonia cooling the surrounding air, resulting in earlier ignition of diesel, resulting in diesel and ammonia being able to burn in a diffusion flame mode. Injecting ammonia at -15 CAD aTDC, and later, shows that diesel is able to ignite and burn as a diffusion flame undisturbed by the ammonia spray, and the ammonia ignites and burns immediately when reaching the diesel flame. The ammonia thereby also burns as a diffusion flame. By delaying the ammonia injection further after -15 CAD aTDC, the ammonia injection overlaps less with the diesel injection, causing less ammonia to be injected into a standing diesel spray flame. This could affect the burnout rate of ammonia since ammonia requires high energy input in order to vaporise, ignite and burn. Figure 12 show the HRR curves for AES 50 %. Very similar trends are found for AES 50 % as found for AES 40 %. The fully premixed mode during the initial stage is also found for AES 50 % close to the same ammonia injection timing as for AES 40 %, i.e. at -22.5 CAD aTDC.

Emissions

The emissions are all presented in molar fractions of the exhaust gas. The wet concentration includes water vapour in the exhaust, which is from the FTIR measurement, while the dry concentration does not include water vapour, which corresponds to the measurements done by the Horiba analyzer, i.e. O2, CO2 and total unburned hydrocarbon (THC).

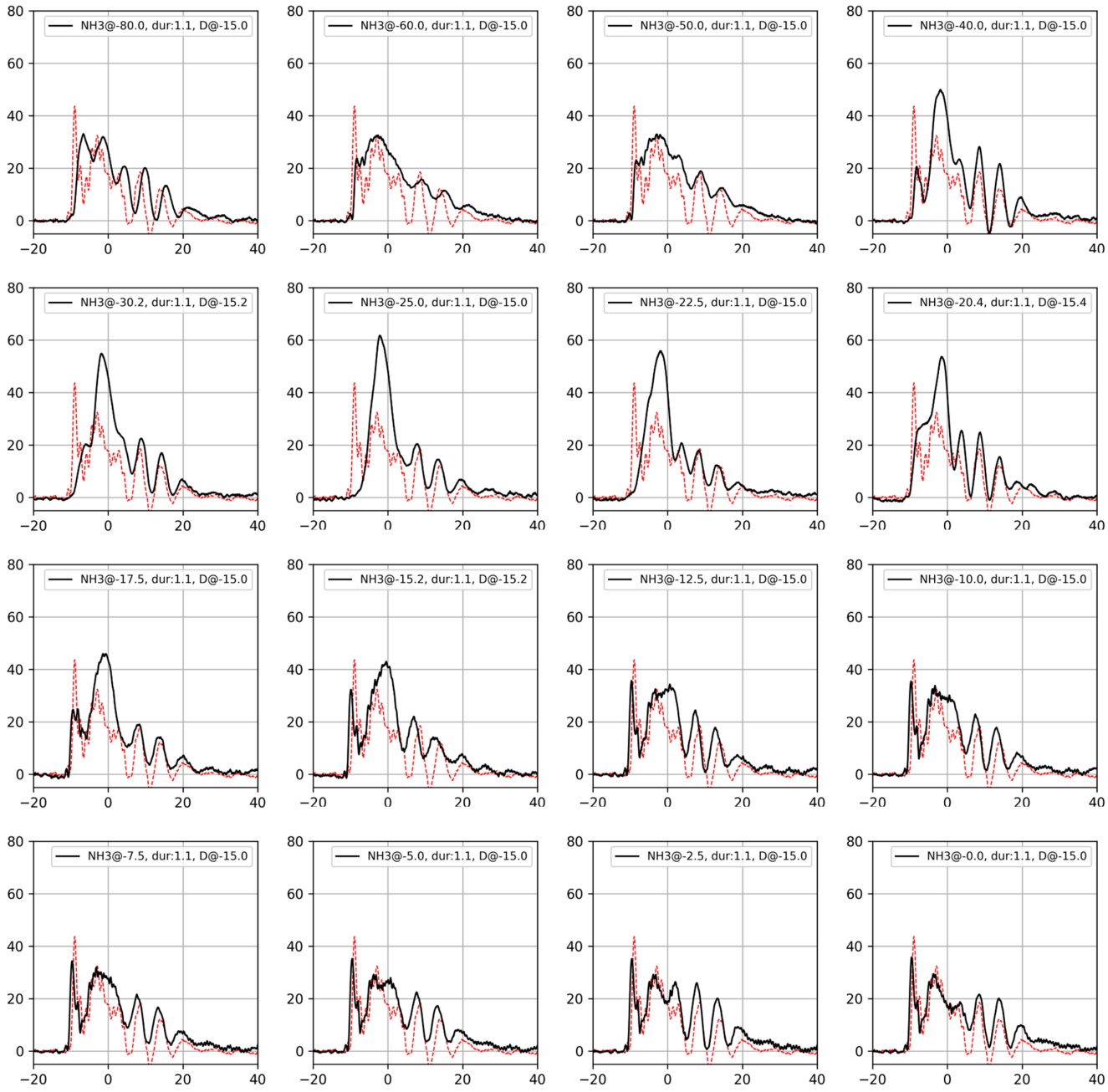

Figure 11: Heat release rate curves for all operating points for 40 % AES. The x-axis shows the heat release rate in joules per CAD, while the y-axis indicates the CAD aTDC. The dotted red curve indicates the diesel-only case.

Figure 14 shows the dry concentrations of O2 and CO2. The oxygen concentration indicates how much fuel was burned, and CO2 indicates how efficiently diesel was combusted. The O2 concentrations correlate well with the heat energy released for each operating point.

The measured ammonia concentrations in the exhaust are shown in Figure 15. For AES 40 % and very early injections of ammonia, high concentrations of ammonia are observed, e.g. 3.8 vol%

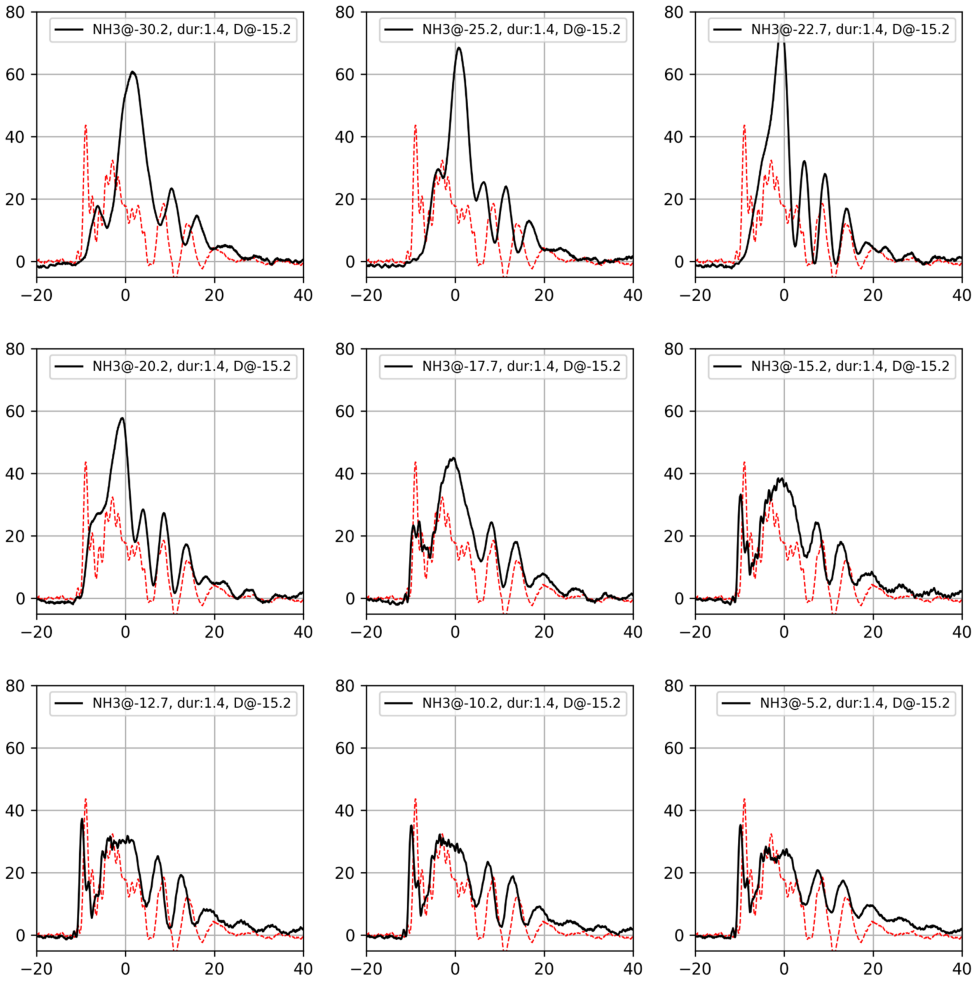

Figure 12: Heat release rate curves for all operating points for 50 % AES. The x-axis shows the heat release rate in joules per CAD, while the y-axis indicates the CAD aTDC. The dotted red curve indicates the diesel-only case.

of the exhaust is ammonia for -80 CAD aTDC. The ammonia concentration gradually decreases as the injection of ammonia is delayed. The minimum ammonia concentration is reached at -15 CAD aTDC, 2200 ppm, i.e. simultaneous injection of ammonia and diesel. For AES 50 %, the minimum ammonia concentration is reached at -20 CAD aTDC, 3780 ppm. The ammonia concentration increases suddenly after -17.5 CAD aTDC and stabilizes at 15000 ppm for later injections of ammonia. The same behaviour is not observed for the AES 40 % case, where the ammonia concentration increases only slightly compared to AES 50 % case.

The concentration of NOx in the exhaust is shown in Figure 16a. All NOx concentrations for ammonia-diesel mode are found to be lower or equal to that of diesel-only mode. The maximum concentration is found for AES 40 % when injecting ammonia at -20 CAD aTDC. The NOx concentration decreases quickly when delaying ammonia injection after -17.5 CAD aTDc, which might be correlated with the degree of premixed combustion taking place. The AES 50 % case shows a similar trend, where the peak is at -25 CAD aTDC, although the peak concentration might not have been captured fully. The peak NOx levels for AES 50 % are also considerably lower than that of AES 40

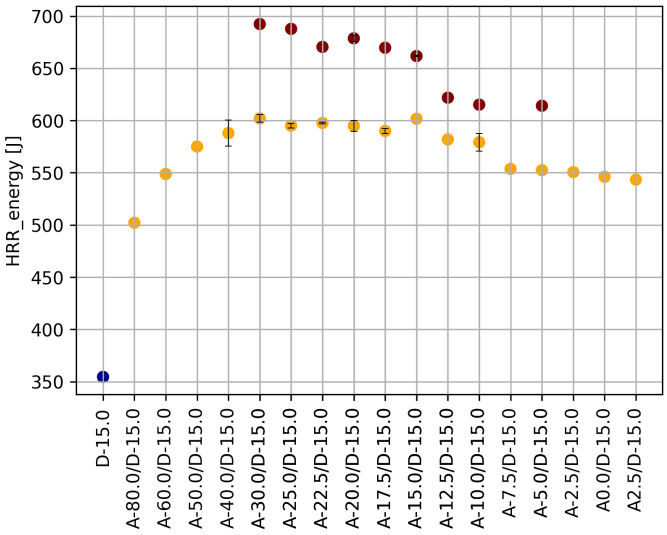

Figure 13: The heat energy released per engine cycle.

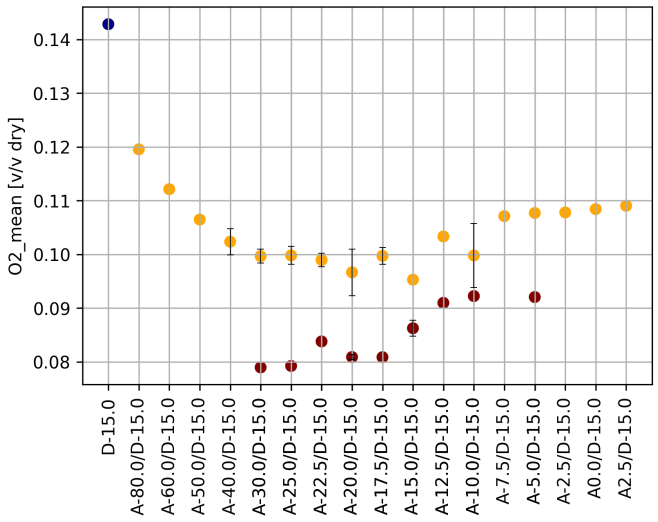

(a) Dry O2 concentration in the exhaust.

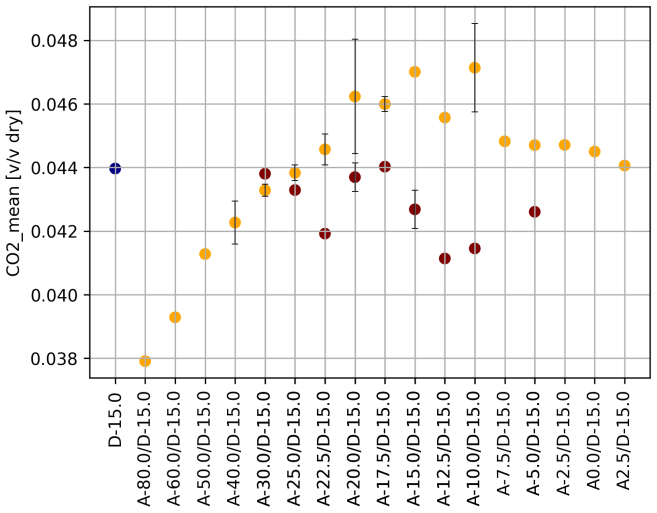

(b) Dry CO2 concentration in the exhaust.

Figure 14: Varying ammonia injection timing while keeping diesel injection timing at -15 CAD aTDC.

%. In Figure 16b the concentration of N2O is shown. Generally, N2O has an opposite trend to NOx, since NOx is determined mainly by high-temperature reactions, leading to the formation of NO, while N2O is produced and nearly fully consumed during the complete combustion of ammonia, a higher emission N2O is therefore related to quenching effects, where N2O is not able to be consumed, caused by cold walls or the vaporizing ammonia spray. The N2O trend for both AES is non-monotonical after ammonia injection timing of -17.5 CAD aTDC, where a sudden increase followed by a decrease is observed. When injecting ammonia at -12.5 and -10 CAD aTDC, a quenching effect might appear, related to the cylinder/piston geometry and injector positioning. This trend is observed for both 40 % and 50 % AES, indicating that it is not caused by experimental uncertainties.

The CO and total hydrocarbon concentrations in the exhaust are shown in Figure 17. CO and THC are both indicative of incomplete hydrocarbon combustion, which could be due to poor combustion of diesel caused by wall impingement or cooling from the ammonia spray. For AES 40

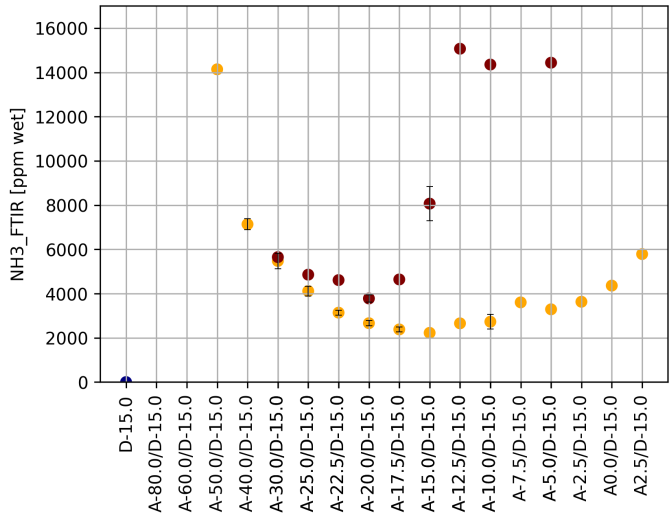

Figure 15: Ammonia concentration in the exhaust. Ammonia injection timing at -80 CAD aTDC: 38000 ppm, -60 CAD aTDC: 27000 ppm.

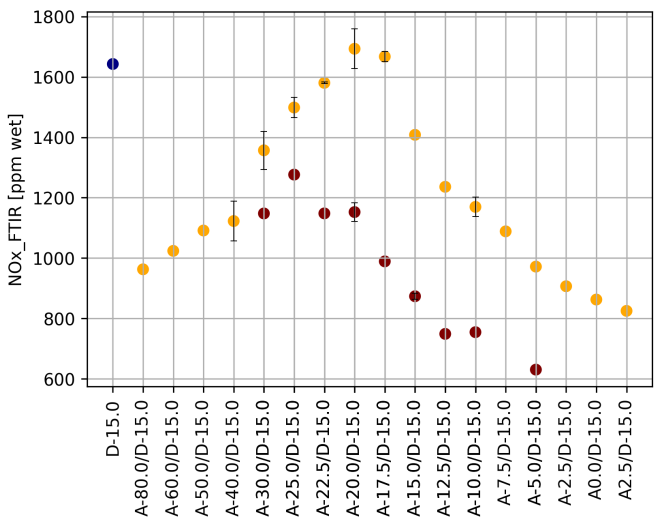

(a) NOx concentration in the exhaust.

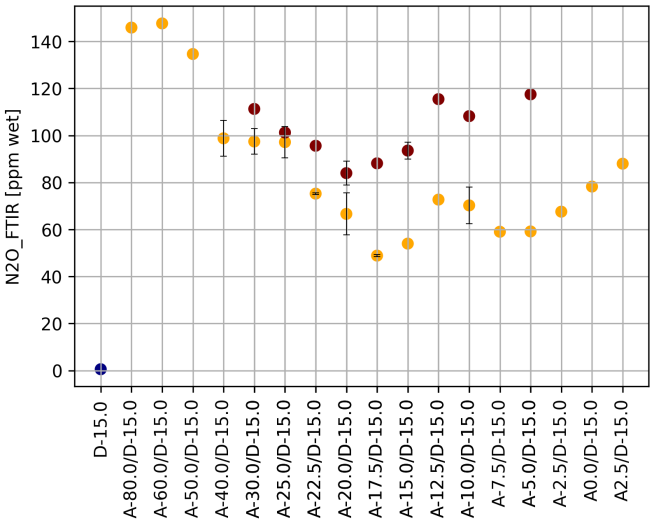

(b) N2O concentration in the exhaust.

Figure 16: Varying ammonia injection timing while keeping diesel injection timing at -15 CAD aTDC.

%, CO is relatively stable. The lowest concentration is found for ammonia injection timing of -17.5 CAD aTDC, and the concentration increases quickly back to a higher level as the injection timing is further delayed. The same is not found for AES 50 % where CO is found to be stable for all ammonia injection timings measured, but the level of CO is much higher.

THC is found to be relatively stable for the earlier ammonia injection timings of AES 40 %, and a slight decrease can be observed for AES 40 % after -20 CAD aTDc. For AES 50 %, a distinct peak is found at -25 CAD aTDc, and similar levels for AES 40 % are observed for injections at -15 CAD aTDC and later. The high THC levels correlate well with the high degree of interaction between ammonia and diesel, causing longer ignition delay times, higher peak pressure variations and a high portion of premixed combustion.

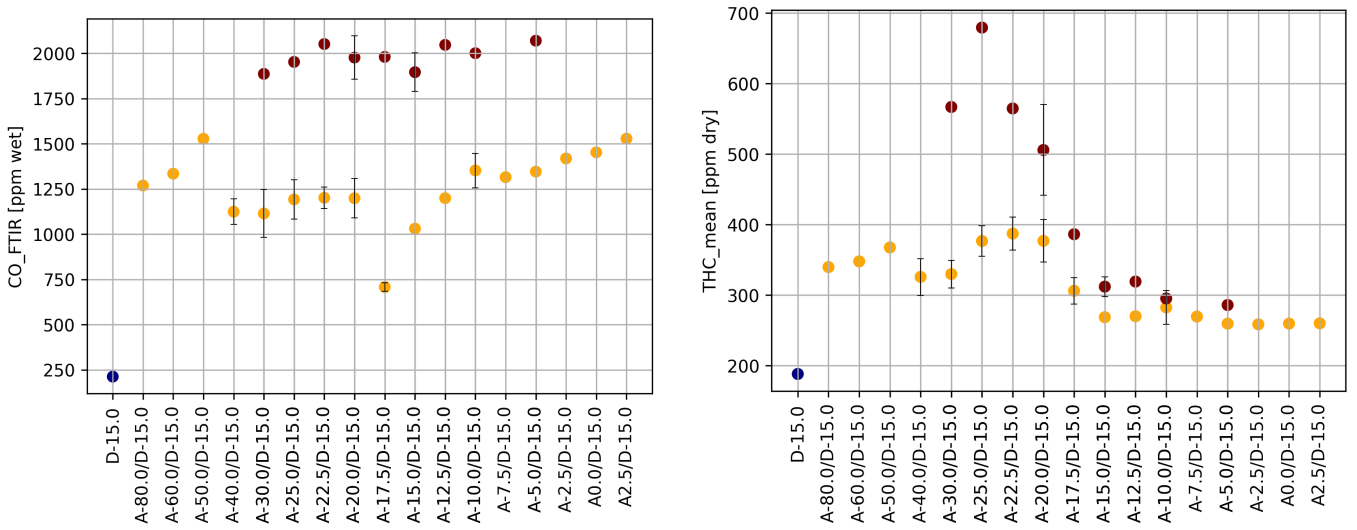

(a) CO concentration in the exhaust.

(b) Total hydrocarbons concentration in the exhaust.

Figure 17: Varying ammonia injection timing while keeping diesel injection timing at -15 CAD aTDC.

3.2 Effect of combustion phasing

A variation of the combustion phasing of the optimal operating point of AES 40 % and 50 % is was performed. For AES 40 %, the optimal operating point was the simultaneous injection of ammonia and diesel fuel, yielding the highest efficiencies and lowest emissions, while for AES 50 %, the optimal point was injecting ammonia/diesel at -20/-15 CAD aTDC. By delaying the combustion phase, the combustion process is occurring at higher temperatures, i.e. closer to TDC. Also, a benefit is achieved thermodynamically since more of the heat is released after TDC, contributing to the indicated power produced.

For AES 40 %, by delaying the injection of ammonia and diesel from -17.5 CAD aTDC to -10 CAD aTDC, while keeping the difference in injection timing the same, the thermal and combustion efficiencies were found to increase from 36.5 % to 40 % and 87.5 % to 90.5 %, respectively. The IMEP COV decreased 1.3 % to 1.15 %, however, the COV of the peak in-cylinder pressure rose from 0.75 % to 1.05 %. The combustion phasing CA10 and CA50 were delayed by approximately 7 degrees, while CA90, indicating the end of combustion, did not change linearly, whereas the -12.5 and -10 CAD aTDC injection timing points had similar positions at 22 CAD aTDC. For AES 50 %, the thermal efficiency also increases when delaying the injections, while the combustion efficiency also increases, but stagnates at ammonia/diesel injection timing of -20/-15 CAD aTDC. Similar to AES 40 %, the CA10 and CA50 increase linearly with delaying the injection timings, while CA90 does not show any clear trend. COV of IMEP is decreased when delaying injection timings, suggesting that more stable power delivery is achieved, while, COV of peak in-cylinder pressure is stable at 0.92 % from -25/-20 to -20/-15 CAD aTDC injection timings, but increase when delaying further.

The emissions measurements show a slight decrease in unburned ammonia in the exhaust when delaying combustion phasing from -17.5 CAD aTDC to -10 CAD aTDC for AES 40 %, while the same is observed for AES 50 %. The NOx emissions decreased from 1630 ppm to 1090 ppm for AES 40 %, and 1590 ppm to 780 ppm for AES 50 %, while N2O increased from 50 ppm to 70 ppm for AES 40 % and 75 ppm to 97 ppm for AES 50 %.

The HRR curves for AES 40 % and 50 % are shown in Figure 18. For the AES 40 %, the injection timing is the same for ammonia and diesel, while for the AES 50 % case, ammonia is injected 5 CAD

before diesel. For AES 40 %, the HRR curves are shifted, following the diesel injection timing, and do not change the shape noteworthy. For AES 50 %, the HRR curves are also shifted related to the delayed injection timings. However, for AES 50 %, the HRR curves' shapes change when shifting the combustion phasing. The premixed combustion phase becomes more distinct when delaying the injections, indicating that the ignition delay time is shortened. For AES 40 %, when changing the ammonia/diesel injection timing -17.5/-17.5 to -10/-10 CAD aTDC, the ignition delay time (defined as the difference between the start of diesel injection and CA10) is shortened by 0.46 CAD (51 μ s) from 8.34 CAD to 7.88 CAD. For AES 50 %, when changing the ammonia/diesel injection timing -22.5/-17.5 to -15/-10 CAD aTDC, the ignition delay time is shortened by 1.78 CAD (198 μ s) from 10.44 CAD to 8.66 CAD. When injecting ammonia 5 CAD before, the ignition delay time is more sensitive to temperature changes in the cylinder.

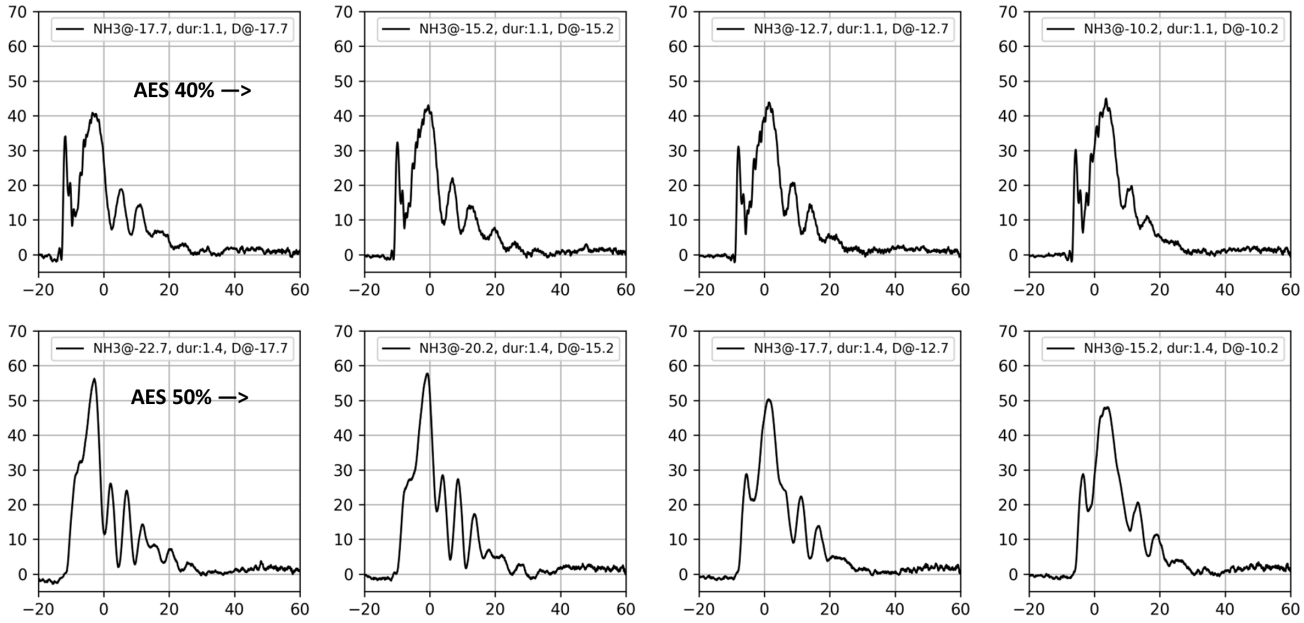

Figure 18: Heat release rate curves for AES 40 % and 50 % for varying combustion phasing. The x-axis shows the heat release rate in joules per CAD, while the y-axis indicates the CAD aTDC.

4 Conclusions

This study concludes the work conducted in WP1 of the ACTIVATE project. A journal publication will follow where all the results will be shared with the scientific community. The work includes the ammonia-diesel engine work conducted in this study, where two ammonia energy shares for 40 and 50 % have been investigated for various ammonia injection timings. The conclusions of the study are as follows:

1. The current study reports the first engine study with ammonia and diesel combustion in HPDF mode with emissions data, including heat release rate curves and combustion efficiencies.

2. For diesel injection timing at -15 CAD aTDC, the thermal and combustion efficiency of AES 40 % increase when delaying the injection of ammonia, reaching a plateau at approximately -30 CAD aTDC. For AES 50%, earlier injection timings of ammonia result in better thermal efficiency (although injections earlier than -30 CAD aTDC were not measured).

3. The COV IMEP values indicate that injecting ammonia slightly before diesel injection results in a more stable power delivery for both AES 40 % and AES 50 %.

4. The COV for the maximum in-cylinder pressure suggests that injecting ammonia at -30 CAD aTDC and -25 CAD aTDC leads to higher cycle-to-cycle variation in peak pressure. Moreover, increasing the AES from 40 % to 50 % exacerbates this instability, as indicated by the increase in COV from 1.5 % to 2.5 % at -25 CAD aTDC.

5. The timing of ammonia injection significantly affects the start of combustion (CA10). Early injection of ammonia (-80 CAD aTDC) delays ignition due to the presence of ammonia and reduced in-cylinder temperature, resulting in a CA10 occurring at -6.5 CAD aTDC, approximately 0.95 ms after the start of diesel injection.

6. The CA10 is further delayed as the injection of ammonia is delayed, reaching a maximum at -25 CAD aTDC for AES 40 % at -4 CAD aTDC, corresponding to 1.22 ms from the start of diesel injection. This peak suggests significant interaction between the ammonia and diesel sprays for these injection timings. The CA10 decreases for later injection timings of ammonia.

7. Injecting ammonia after the start of diesel injection (after -15 CAD aTDC) results in unaffected ignition of diesel, but the CA10 is still delayed by 1 CAD for AES 40 % and 2 CAD for AES 50 % compared to diesel alone. This delay can be attributed to the impact of previous combustion cycles on the conditions in the cylinder.

8. Injecting ammonia at -60 and -40 CAD aTDC leads to a premixed combustion phase followed by a diffusion-based flame. This suggests that the ammonia has enough time to mix and vaporize in the air before diesel injection, resulting in the ignition of the mixture.

9. The premixed combustion mode observed for -25 and -22.5 CAD aTDC ammonia injection timings is caused by a delayed start of ignition and results in a high heat release rate (HRR) peak.

10. Delaying the injection of ammonia decreases the unburned ammonia concentration in the exhaust. Minimum concentrations are observed at -15 CAD aTDC for AES 40 % and -20 CAD aTDC for AES 50 %. Later injection timings result in a significant increase in ammonia concentration, particularly for AES 50 %.

11. Peak NOx levels occur at different ammonia injection timings for AES 40 % and AES 50 %, i.e. -20 CAD aTDC and -25 CAD aTDC, respectively. Delaying the ammonia injection reduces NOx concentration. AES 50 % shows a lower peak NOx level than AES 40 %.

12. The N2O concentration shows an opposite trend from NOx, where the minimum is found at -17.5 and -20 CAD aTDC for AES 40 % and 50 %, respectively. N2O exhibits a non-monotonic trend after -17.5 CAD aTDC for both AESs, possibly indicating geometrically driven quenching effects.

13. The concentration of CO and total hydrocarbons (THC) in the exhaust indicates incomplete hydrocarbon combustion. For AES 40 %, CO remains relatively stable, with the lowest concentration observed at -17.5 CAD aTDC. For AES 50 %, CO levels are consistently higher and stable across all measured injection timings.

14. THC concentration shows stability for early ammonia injection timings in AES 40 %, with a slight decrease after -20 CAD aTDC. In contrast, AES 50 % exhibits a distinct peak in THC concentration at -25 CAD aTDC, similar to the levels observed for AES 40 % at -15 CAD aTDC and later injection timings. The higher THC levels correspond to increased interaction between liquid ammonia and diesel, leading to poorer combustion of diesel.

15. Delaying the ammonia/diesel injection timing to -10/-10 CAD aTDC for 40 % AES and to -20/-15 CAD aTDC for 50 % AES, positively affects engine performance and emissions.

Norway grants

References

[1] Stephanie Frankl, Stephan Gleis, Stephan Karmann, Maximilian Prager, and Georg Wachtmeister. Investigation of ammonia and hydrogen as CO2-free fuels for heavy duty engines using a high pressure dual fuel combustion process. *International Journal of Engine Research*, 22(10):3196–3208, October 2021. Publisher: SAGE Publications.

[2] Tie Li, Xinyi Zhou, Ning Wang, Xinran Wang, Run Chen, Shiyan Li, and Ping Yi. A comparison between low- and high-pressure injection dual-fuel modes of diesel-pilot-ignition ammonia combustion engines. *Journal of the Energy Institute*, 102:362–373, June 2022.

[3] Valentin Scharl and Thomas Sattelmayer. Ignition and combustion characteristics of diesel piloted ammonia injections. *Fuel Communications*, 11:100068, June 2022.

[4] Valentin Scharl, Tomislav Lackovic, and Thomas Sattelmayer. Characterization of ammonia spray combustion and mixture formation under high-pressure, direct injection conditions. *Fuel*, 333:126454, February 2023.

[5] Zhenxian Zhang, Wuqiang Long, Pengbo Dong, Hua Tian, Jiangping Tian, Bo Li, and Yang Wang. Performance characteristics of a two-stroke low speed engine applying ammonia/diesel dual direct injection strategy. *Fuel*, 332:126086, January 2023.